
ADAPTIVE k -NEAREST NEIGHBOR CLASSIFIER BASED ON THE LOCAL ESTIMATION OF THE SHAPE OPERATOR

Alexandre Luís Magalhães Levada *
Federal University of São Carlos
13565-905, São Carlos-SP, Brazil
alexandre.levada@ufscar.br

Frank Nielsen
Sony Computer Science Laboratories
141-0022, Tokyo, Japan
frank.nielsen.x@gmail.com

Michel Ferreira Cardia Haddad
Queen Mary University of London
E1 4NS, London, United Kingdom
m.haddad@qmul.ac.uk

September 10, 2024

ABSTRACT

The k -nearest neighbor (k -NN) algorithm is one of the most popular methods for nonparametric classification. However, a relevant limitation concerns the definition of the number of neighbors k . This parameter exerts a direct impact on several properties of the classifier, such as the bias-variance tradeoff, smoothness of decision boundaries, robustness to noise, and class imbalance handling. In the present paper, we introduce a new adaptive k -nearest neighbours (kK -NN) algorithm that explores the local curvature at a sample to adaptively defining the neighborhood size. The rationale is that points with low curvature could have larger neighborhoods (locally, the tangent space approximates well the underlying data shape), whereas points with high curvature could have smaller neighborhoods (locally, the tangent space is a loose approximation). We estimate the local Gaussian curvature by computing an approximation to the local shape operator in terms of the local covariance matrix as well as the local Hessian matrix. Results on many real-world datasets indicate that the new kK -NN algorithm yields superior balanced accuracy compared to the established k -NN method and also another adaptive k -NN algorithm. This is particularly evident when the number of samples in the training data is limited, suggesting that the kK -NN is capable of learning more discriminant functions with less data considering many relevant cases.

1 Introduction

The k -nearest neighbor classifier (k -NN) is a nonparametric method known for its simplicity, versatility, and intuitive approach to classification tasks [Cover and Hart, 1967, Nielsen, 2016]. The k -NN algorithm is well-suited to handling complex, non-linear relationships and high-dimensional datasets where the underlying structure may be difficult to specify [Zhang, 2022]. Another advantage refers to its ease of implementation and interpretability, being the classification decision determined by the majority class among the k -nearest neighbors of a given data point. Moreover, the k -NN classifier requires minimal training time since it essentially memorizes the training dataset, becoming suitable for both online and offline learning scenarios. Furthermore, the k -NN algorithm adapts dynamically to changes within the dataset, being more robust to noise and outliers [Syriopoulos et al., 2023].

The parameter k controls the neighborhood size, playing a crucial role in determining behavior and performance of the k -NN classifier. This parameter represents the number of nearest neighbors considered when making predictions for a new data point [Jodas et al., 2022]. A smaller k value leads to a more flexible model with decision boundaries that closely follow the training data, potentially capturing intricate patterns and local variations. However, smaller k values may increase the susceptibility to noise and outliers, due to the fact that it excessively relies on the nearest neighbors

for classification [Uddin et al., 2022]. Conversely, larger k values result in a smoother decision boundary and a more generalized model that is less affected by individual data points. Nonetheless, exceedingly large k values may cause the model to overlook local patterns, resulting in an inferior performance - notably in datasets with complex structures. Therefore, selecting the appropriate k value is pivotal for achieving an appropriate balance between bias and variance, ensuring optimal generalization and predictive accuracy on testing or new data. The parameter k is commonly the same for all samples in the dataset [Batista and Silva, 2009].

The motivation of the present work is to improve the performance of the k -NN classifier through the incorporation of a geometric property (local curvature) in the definition of the neighborhood size. A high curvature sample \vec{x}_i should have a smaller neighborhood, as the patch P_i composed by \vec{x} and its closest neighbors deviates from a linear subspace, being the patch P_i defined as the set $\{\vec{x}_i, \vec{x}_{i1}, \dots, \vec{x}_{ik}\}$. Conversely, low curvature samples should have larger neighborhoods, as the patch P_i is approximately linear. Several works investigated the incorporation of distance functions and adaptive approaches to define the parameter k dynamically for each dataset [Abu Alfeilat et al., 2019, Zhao and Lai, 2021, Papanikolaou et al., 2021, Daulay et al., 2023]. Techniques for the local adaptive estimation of the neighborhood size for each sample of a dataset have been proposed for the k -NN classifier [Sun and Huang, 2010, Fan et al., 2023]. Notwithstanding, most of the literature adopts the optimization of a local criterion to choose the best value of k from a list of candidates.

In the present paper, we introduce an adaptive curvature based k -nearest neighbor classifier to automatically adjust the number of neighbors for each sample of a dataset. The proposed method is named kK -NN due to the fact that it consists of an k -NN method with k varying locally according to the Gaussian curvature. The intuition behind the kK -NN classifier is to explore the local curvature to define the size of the neighborhood k at each vertex of the k -nearest neighbors graph (k -NNG) in an adaptive manner. As detailed in Algorithm 1, in the case of points with lower curvature values, the tangent plane is commonly closely adjusted to a manifold. The kK -NN classifier is composed by the training and testing stages (algorithms 2 and 3, respectively). In the training stage, the first step consists of building the k -NNG from the input feature space using $k = \log_2 n$, where n is the number of samples. Subsequently, it is computed the curvature of all vertices of the k -NNG exploring the shape operator-based algorithm. The curvatures are then quantized into ten different scores. Considering that the scores are based on the local curvatures, the adaptive neighborhood adjustment is performed by pruning the edges of the k -NNG.

There are three main contributions of the proposed kK -NN algorithm. Firstly, transforming the number of neighbors spatially-invariant along a k -NN graph in order to avoid both underfitting and overfitting. Secondly, to control the smoothness of the decision boundaries, depending on the local density in the feature space. Thirdly, to improve the robustness to noise and outliers through the identification of high curvature points adopting an approximation for the local shape operator of the data manifold [do Carmo, 2017, Needham, 2021, Boissonnat and Wintraecken, 2022]. Computational experiments with 30 real-world datasets indicate that the proposed kK -NN classifier is capable of improving the balance accuracy compared to the existing k -NN and another competing adaptive k -NN algorithm proposed in LeJeune et al. [2019], especially while dealing with small training datasets.

The results indicate that the kK -NN classifier is consistently superior compared to the regular k -NN and also the competing adaptive k -NN algorithm. The rationale behind the capacity of the kK -NN to improve the regular kk -NN may be summarized by three relevant aspects. Firstly, through the use of an adaptive strategy to define the neighborhood sizes, the kK -NN is capable of avoiding either underfitting or overfitting. Secondly, in more dense regions the decision boundaries becomes more adjusted to the samples, while in less dense regions the boundaries become smoother - making the classification rule adaptive to different regions of the feature space. Thirdly, high curvature points are commonly related to outliers, being the kK -NN classifier capable of isolating such samples by drastically reducing its neighborhoods. It is worth mentioning that the kK -NN classifier is capable of learning more discriminant decision functions when the number of training samples is considerably reduced. These results suggest that the kK -NN algorithm may provide more flexible and adjustable decision boundaries, while reducing the influence of outliers over the classification process.

The remainder of the paper is organized as follows. Section 2 presents the proposed adaptive curvature-based kK -NN classifier. Section 3 reports computational experiments and results. Section 4 concludes and suggests future research possibilities. The appendices provide further details on the shape operator, curvatures, and the regular k -NN classifier.

2 Adaptive curvature based k -NN classifier

One of the main limitations of the k -NN classifier refers to its parameter sensitivity, as the performance of the k -NN is highly dependent upon the choice of the parameter k - i.e., the number of nearest neighbors being considered. Selecting an inappropriate value of k may result in a series of negative effects to its performance such as [Zhang, 2022, Syriopoulos et al., 2023, Daulay et al., 2023]:

- **Overfitting and underfitting:** The parameter k controls the flexibility of the decision boundary of the k -NN classifier. A smaller value of k yields a more flexible (less smoothing) decision boundary, which may lead to overfitting - particularly in noisy or high variance datasets. Conversely, a larger value of k results in a smoother decision boundary, which may lead to underfitting and inappropriate generalization in the case that the k is excessively large compared to the dataset size or the underlying structure of the data.
- **Bias-variance tradeoff:** The choice of k in the k -NN classifier involves a trade-off between bias and variance. A smaller k leads to low bias and high variance. This means that the classifier might capture more complex patterns in the data, although it is sensitive to noise and fluctuations. On the other hand, a larger k reduces variance while increases bias, potentially leading to simpler decision boundaries that may not capture the true underlying structure of the data.
- **Robustness:** The sensitivity of the k -NN classifier to the k parameter affects its robustness to noisy data points and outliers. A larger k may mitigate the effects of noise by considering a larger number of neighbors, whereas a smaller k may lead to overfitting - in which case the classifier is more affected by noisy data points.
- **Impact on class-imbalanced data:** The minority class (i.e., a class with fewer instances) tends to be underrepresented compared to the majority class. The choice of the k parameter may influence the classification of minority class instances. A smaller k may result in the majority class dominating the prediction for the minority class instances. Since the nearest neighbors are predominantly from the majority class, the minority class observations might be misclassified or even ignored. A larger k may incorporate more neighbors, potentially improving the representation of the minority class. However, it might also introduce noise from the majority class, leading to misclassification of minority class observations.

2.1 Algorithm to estimate the shape operator curvature

In order to propose our method to compute Gaussian curvatures, suppose that $X_i = \{\vec{x}_1, \dots, \vec{x}_n\}$, where $\vec{x}_i \in \mathbb{R}^m$, denotes the input of the data matrix, in which each column of X_i represents a sample of the dataset. Given matrix X_i , we may build a graph from the k -nearest neighbors of each sample (*k-nearest neighbor graph*), known as k -NNG. For each sample, calculate its k -nearest neighbors based on a distance metric (e.g., Euclidean distance, Manhattan distance) in the feature space. Then, include an edge linking each sample to its k -nearest neighbors, preparing a graph where each sample is a node, which edges represent the connections between a pair of nodes [Eppstein et al., 1997]. An example of a k -NNG created using a real-world dataset is illustrated in Figure 1.

The k -NNG in Figure 1 adopts the Euclidean distance in the computation of the nearest neighbors of each sample \vec{x}_i . Let η_i be the k nearest neighbors of \vec{x}_i . Then, a patch P_i may be defined as the set $\{\vec{x}_i, \vec{x}_{i1}, \dots, \vec{x}_{ik}\}$. It is worth noticing that the cardinality of this set is $k + 1$. In matrix notation, the patch P_i is given by:

$$P_i = \begin{bmatrix} x_i(1) & x_{i1}(1) & \dots & x_{ik}(1) \\ x_i(2) & x_{i1}(2) & \dots & x_{ik}(2) \\ \vdots & \vdots & \ddots & \vdots \\ \vdots & \vdots & \dots & \vdots \\ x_i(m) & x_{i1}(m) & \dots & x_{ik}(m) \end{bmatrix}_{m \times (k+1)} \quad (1)$$

In the proposed method, we approximate the local metric tensor at a point \vec{x}_i as the inverse of the local covariance matrix, Σ_i^{-1} , estimated from the patch P_i . Our motivations for this choice are listed below, following [Li and Tian, 2018, Wang and Sun, 2015, Hair-Jr. et al., 2018]:

- **Positive-definiteness:** The covariance matrix is positive-definite, implying that it defines a positive-definite inner product on the space of the data. Similarly, its inverse retains this property, ensuring that it represents a valid metric tensor.
- **Measurement of distances:** The elements of the inverse covariance matrix (i.e., precision matrix) provide information about the distances between points in the feature space. A larger value in the inverse covariance matrix indicates a smaller distance between the corresponding features, while a smaller value indicates a larger distance. This information reflects the relationships and correlations between features in the dataset.
- **Directional sensitivity:** Similarly to a metric tensor in differential geometry, the inverse covariance matrix is sensitive to changes in the direction within the feature space. It quantifies how distances between points change as one moves along different directions in the space, capturing the curvature and geometry of the data manifold.

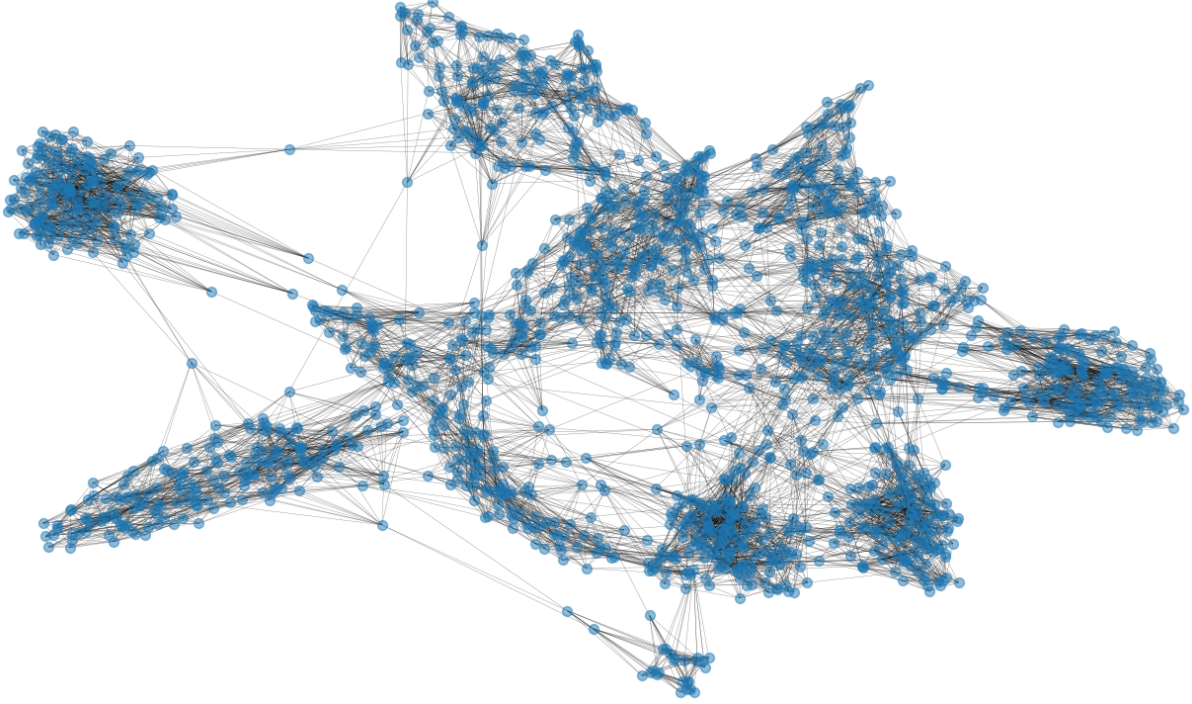


Figure 1: The k -NNG of a dataset of handwritten digits with $n = 1797$ samples (graph nodes) and $k = \log_2 n$ neighbors.

- **Mahalanobis distance:** The inverse covariance matrix is closely related to the Mahalanobis distance, which is a non-isotropic distance between vectors, considering the correlations between features. The role of the inverse covariance matrix in the Mahalanobis distance is to allowing different degrees of deformations of the space. It has been applied in many statistical and machine learning problems related to outlier detection, clustering, and classification.

Hence, a discrete approximation for the metric tensor (first fundamental form) at \vec{x}_i is given by the inverse of the local covariance matrix Σ_i :

$$\Sigma_i = \frac{1}{k} \sum_{x_j \in P_i} (\vec{x}_j - \vec{x}_i)(\vec{x}_j - \vec{x}_i)^T \quad (2)$$

where \vec{x}_i is the central sample. Our approximation consists in setting the first fundamental form of a surface at a given point \vec{x}_i as $\mathbb{I}_i \approx \Sigma_i^{-1}$ for every sample in the k -NNG.

To compute a discrete approximation for the curvature tensor (second fundamental form) of a surface, we use a mathematical result that states that \mathbb{II} is related to the Hessian matrix through the parametrization of the surface, and the scalar-valued function representing the surface itself. The coefficients of the second fundamental form may be expressed in terms of the second partial derivatives of the components of the surface parametrization function. The second fundamental form is then proportional to the Hessian, which is the matrix of second order partial derivatives [Kuhnel, 2015]¹. Our approach is based in the strategy adopted by the manifold learning algorithm known as Hessian eigenmaps [Donoho and Grimes, 2003]. Considering the case of $m = 2$ - meaning that the feature vectors are 2D, the X_i is defined as the matrix composed by the following columns:

$$X_i = [1, U_1, U_2, U_1^2, U_2^2, (U_1 \times U_2)] \quad (3)$$

where U_i denotes the i -th eigenvector of the local covariance matrix, computed from the samples belonging to the patch P_i . The notation $U_i \times U_j$ denotes the pointwise product between vectors U_i and U_j .

¹For the interested reader, further details about the first and second fundamental forms of surfaces are provided in Chase [2012]

When $m > 2$, the matrix X_i must have $1 + m + m(m + 1)/2$ columns, in which the first column is a vector of 1's, the next m columns are the eigenvectors of Σ_i , and the final $m(m + 1)/2$ columns are the square eigenvectors followed by the several cross products between them. For example, if $m = 3$, the matrix X_i is given by:

$$X_i = [1, U_1, U_2, U_3, U_1^2, U_2^2, U_3^2, (U_1 \times U_2), (U_1 \times U_3), (U_2 \times U_3)] \quad (4)$$

Matrix H_i is then defined as the matrix with the last $m(m + 1)/2$ columns of X_i transposed:

$$(H_i)_{r,l} = (\tilde{X}_i)_{l,1+m+r} \quad (5)$$

A final step consists of transforming the Hessian estimator into a square $m \times m$ matrix. The local second fundamental form at sample \vec{x}_i , denoted by \mathcal{H}_i , is then given by:

$$\mathcal{H}_i = H_i H_i^T \quad (6)$$

Our approximation becomes $\mathbb{I}_i \approx \mathcal{H}_i$. Both estimators for \mathbb{I} and \mathbb{III} are square $m \times m$ matrices. Lastly, our approximation to the local shape operator at \vec{x}_i is given by:

$$\mathcal{S}_i = -\mathbb{III}_i(\mathbb{I}_i)^{-1} = -\mathcal{H}_i \Sigma_i \quad (7)$$

Thus, the determinant of \mathcal{S}_i is the desired Gaussian curvature at point \vec{x}_i . With the proposed method, it is possible to assign a curvature for each sample of the dataset. The pseudocode of the proposed shape operator curvature estimation method is detailed in algorithm 1.

Algorithm 1 Shape operator-based curvatures

```

function SHAPE-OPERATOR-CURVATURES( $X_i, k$ )
  //  $X_i$ : the  $n \times m$  data matrix (each row is a sample)
  //  $k$ : the number of neighbors in the  $k$ NN-graph
   $A \leftarrow k$ NN-graph( $X_i, k$ )                                     ▷ Builds the  $k$ NN-graph
  for  $i \leftarrow 1; i < n; i++$  do
    neighbors  $\leftarrow N(\vec{x}_i)$                                        ▷ Neighborhood of sample  $\vec{x}_i$ 
     $\Sigma_i \leftarrow$  cov-matrix(neighbors)                             ▷ Local covariance matrix
     $U \leftarrow$  eigenvectors( $\Sigma_i$ )                                   ▷ Eigenvectors = columns of U
    Compute the matrix  $X_i$  with  $1 + m + m(m + 1)/2$  columns
    Compute the matrix  $H_i$ : the last  $m(m + 1)/2$  columns of  $X_i$ 
     $\mathcal{H}_i \leftarrow \hat{H}_i \hat{H}_i^T$                                          ▷ Second fundamental form
     $\mathcal{S}_i \leftarrow -\mathcal{H}_i \Sigma_i$                                        ▷ Shape operator
     $K_i \leftarrow \det(\mathcal{S}_i)$                                            ▷ Curvature at point  $\vec{x}_i$ 
  end for
  return  $K$                                                          ▷ Vector of curvatures
end function

```

2.2 Curvature-based kK -NN classifier

The intuition behind the new kK -NN classifier is to explore the local curvature to define the size of the neighborhood k at each vertex of the k -NNG in an adaptive fashion. In the case of points with lower curvature values, the tangent plane tend to be tightly adjusted to a manifold as the geometry is relatively flat in the neighborhood of that point. This means that a larger parameter k should be considered. Conversely, points with high curvature values lead to a relevant bending or deformation of the manifold. In such cases, it is challenging to perform an accurate approximation with a flat tangent plane. The tangent plane may be loosely adjusted to the surface in these regions, meaning that a smaller parameter k should be considered.

The kK -NN classifier is composed by two phases, namely training and testing. In the training stage, the first step consists in building the k -NNG from the input feature space using $k = \log_2 n$, where n is the number of samples. Then, the curvature of all vertices of the k -NNG is computed using the shape operator based algorithm detailed in the previous section.

Subsequently, the curvatures are quantized into 10 different scores - from zero to nine. Given the scores based on the local curvatures, the adaptive neighborhood adjustment is performed by pruning the edges of the k -NNG. Suppose that $k = 11$, and the curvature score of sample \vec{x}_i is $c_i = 4$. The edges linking sample \vec{x}_i with its four farthest neighbors would then be disconnected, reducing the neighborhood to only seven neighbors. In the case of $k < c_i$, the sample \vec{x}_i remains connected to its nearest neighbor. In the testing stage, the new sample \vec{z}_i is included to be classified by the k -NNG, linking it to its k -nearest neighbors and computing its local curvature. The curvature of the new point is then added into the curvatures vector, generating its curvature score c_i through a quantization process.

Algorithm 2 kK -NN classifier training

```

function  $kK$ NN-TRAIN(train_set, train_labels,  $k$ )
    curvatures  $\leftarrow$  Shape-Operator-Curvatures(train_set,  $k$ )
    return curvatures
end function

```

The quantization process is executed through algorithm 1, taking the input matrix X_i and the parameter k , while returning an output vector with estimated curvature of each sample (i.e., row of matrix X_i). The curvatures are normalized considering the interval $[0, 1]$. Thus, nine equally spaced subdivisions are generated considering the interval $0.1, \dots, 0.9$. Those nine subdivisions correspond to the quantiles that are calculated, where the quantile 0.0 refers to the smallest curvature value of zero whereas the quantile 1.0 represents the largest curvature value of one. The discrete curvature values (curvature scores) are then found, returning the indices of the bins of their corresponding curvature values. Lastly, its farthest $k - c_i$ neighbors are pruned while assigning the most frequent label in the adjusted neighborhood.

The pseudocode for the training stage of the proposed kK -NN classifier is presented in algorithm 2. The computational complexity of the function kK -NN training is equivalent to the complexity of the function to compute the curvatures using local shape operators. Subsequently, the pseudocode for the testing stage of the kK -NN classifier is detailed in algorithm 3.

Algorithm 3 kK -NN classifier testing

```

function  $kk$ NN-TEST(test_samples, train_labels, curvatures,  $k$ )
     $n \leftarrow$  size(test_samples)
    predictions  $\leftarrow$  zeros( $n$ )
    for  $i \leftarrow 0; i < n; i++$  do
        patch  $\leftarrow$  Find_Neighbors(test_samples[ $i$ ],  $k$ )
        new_curvature  $\leftarrow$  Shape-Operator-Curvatures(patch,  $k$ )
        curvatures  $\leftarrow$  concatenate(curvature, new_curvature)
        scores  $\leftarrow$  quantize(curvatures, 10)
        new_score  $\leftarrow$  scores[-1] ▷ Last score is from the new test sample
        neighborhood  $\leftarrow$  Adjust_Neighbors(patch, new_score)
        predictions[ $i$ ]  $\leftarrow$  Majority_Vote(train_labels[neighborhood])
    end for
    return predictions
end function

```

In the Shape-Operator-Curvatures algorithm, the main loop iterates n times, where n is the number of samples in the training set. The complexity of selecting the k -nearest neighbors is $O(nmk)$, where m is the dimensionality. The cost of the computation of the covariance matrix computation is $O(nm^2)$, while the regular eigendecomposition methods amounts to a cost of $O(m^3)$. The cost of the regular matrix product between two $m \times m$ matrices is $O(m^3)$, and the computation of the determinant of an $m \times m$ matrix is also $O(m^3)$. Therefore, the total cost for the proposed shape operator-based algorithm for curvature computation is:

$$O(n^2mk) + O(n^2m^2) + O(nm^3) \quad (8)$$

which alternatively may be expressed as $O(nm(nk + nm + m^2))$. In general, as $k = \log n < m$ when $n > m$, then the overall cost is $O(n^2m^2)$. If $m > n$, then the overall cost becomes $O(nm^3)$. Comparatively, the computational complexity of the regular k -NN prediction according (Algorithm 4) is $O(mn \log n + mk)$, where n is the number of samples, m is the number of features, and k is the number of neighbors. Due to the presence of a sorting procedure, it is possible to perform a k -NN prediction in $O(n(m + k))$. In practice, the complexity analysis reveals that the proposed algorithm scales better to an arbitrary increase in the number of samples compared to an arbitrary increase in the number

of features. Thus, a dimensionality reduction method such as principal component analysis (PCA) might be required before the computation of the local curvatures for datasets with a large number of features.

The computational complexity of the function kK -NN-test is also dominated by the computation of the curvatures. The function Shape-Operator-Curvatures algorithm performs the computation of the curvature of a simple point. Nonetheless, due to the fact that is inside a “for loop” of size n , the global cost is equivalent to the function employed in the training stage. In comparison with the regular k -NN and the adaptive k -NN, the proposed kK -NN classifier shows a higher computational cost. However, as reported in the subsequent sections, the new kK -NN classifier is capable of improving the classification performance in several datasets, particularly when the number of samples in the training set is limited. The fact that the bottleneck of the kK -NN classifier is the curvature estimation algorithm may be considered as a caveat of the proposed method.

3 Results

Extensive computational experiments are performed to compare the balanced accuracy, Kappa coefficient, Jaccard index, and F1-score of the proposed adaptive kK -NN classifier against the regular k -NN and a further competing adaptive k -NN algorithm [LeJeune et al., 2019]. This competing algorithm performs an adaptive estimation of the distances, exploiting the fact that finding a set of the k nearest neighbors does not require computing their exact corresponding distances. Several real-world datasets are collected from the public repository `openml.org`. The title, sample size, number of features, and number of classes of the 30 datasets used in the first round of experiments are detailed in Table 1. Those datasets cover a wide range of sample sizes, number of features, and classes from many domains.

Table 1: Sample size, number of features, and classes of the selected openML datasets of the first round of experiments.

#	Dataset	# samples	# features	# classes
1	vowel	990	13	11
2	zoo	101	16	7
3	thyroid-new	215	5	3
4	lawsuit	264	4	2
5	arsenic-male-bladder	559	4	2
6	tecator	240	124	2
7	sonar	208	60	2
8	ionosphere	351	34	2
9	prnn_crabs	200	7	2
10	monks-problem-1	556	6	2
11	diggle_table_a2	310	8	9
12	user-knowledge	403	5	5
13	tic-tac-toe	958	9	2
14	parkinsons	195	22	2
15	glass	214	9	6
16	breast-tissue	106	9	4
17	Smartphone-Based_Recognition	180	66	6
18	FL2000	67	15	5
19	fishcatch	158	7	2
20	biomed	209	8	2
21	kidney	76	6	2
22	anneal	898	38	5
23	mfeat-fourier (25%)	500	76	10
24	mfeat-karhunen (25%)	500	64	10
25	letter (10%)	2000	16	26
26	satimage (25%)	1607	36	6
27	pendigits (25%)	2748	16	10
28	texture (25%)	1375	40	11
29	digits (25%)	449	64	10
30	Olivetti_Faces (10 LDA features)	400	10	40

In the first round of experiments, it is adopted a holdout strategy to divide the samples into the training and test datasets. The training partition varies from 10% to 90% of the total samples, using increments of 5% - leading to a total of 17

possible divisions in training and testing stages. The number of neighbors in the regular k -NN is defined as $k = \log_2(n)$, where n is the number of samples. This is the same value used in the proposed kK -NN method.

All three competing algorithms are trained in each one of the 17 training sets, while testing them in the respective test partition. The median balanced score, Kappa coefficient, Jaccard index, and F1-score are computed over the 17 executions. The objective is to test the behavior of the classifier in all scenarios - small, medium, and large training datasets.

The results are reported in Table 2. Considering all evaluation metrics, the proposed kK -NN classifier provides the best results in 19 cases (63% of the datasets), the competing adaptive k -NN algorithm is the best algorithm of 11 cases (37% of the datasets), and the regular k -NN is outperformed in all datasets. These results indicate a superior performance not only on the relatively unsophisticated k -NN but also over a competing adaptive k -NN classifier. A limitation of the proposed kK -NN method refers to its comparatively higher computational cost.

Table 2: Median of measures after 17 executions adopting the holdout strategy with training datasets of different sizes: from 10% to 90% of the number of samples with increments of 5%

Dataset	k -NN				Adap. k -NN				kK -NN			
	Bal. Acc.	Kappa	Jaccard	F1	Bal. Acc.	Kappa	Jaccard	F1	Bal. Acc.	Kappa	Jaccard	F1
1	0.5314	0.4679	0.3430	0.4978	0.6870	0.6620	0.5390	0.6932	0.8860	0.8732	0.7999	0.8828
2	0.5622	0.6898	0.6592	0.7136	0.7917	0.8500	0.8116	0.8660	0.8809	0.9113	0.8924	0.9337
3	0.7525	0.7077	0.8039	0.8840	0.7952	0.7926	0.8454	0.9128	0.8746	0.8628	0.8927	0.9417
4	0.5555	0.1889	0.8701	0.9070	0.7777	0.6996	0.9387	0.9653	0.8758	0.7517	0.9382	0.9662
5	0.5000	0.0000	0.9137	0.9354	0.6666	0.4846	0.9298	0.9556	0.7884	0.6095	0.9354	0.9599
6	0.7779	0.5698	0.6479	0.7843	0.8481	0.7095	0.7499	0.8564	0.8308	0.6689	0.7142	0.8333
7	0.7227	0.4547	0.5712	0.7240	0.8075	0.6154	0.6787	0.8085	0.8285	0.6599	0.7121	0.8315
8	0.7326	0.5146	0.6568	0.7839	0.7826	0.6194	0.7083	0.8241	0.8205	0.6824	0.7484	0.8534
9	0.8097	0.6196	0.6806	0.8099	0.8562	0.7113	0.7474	0.8555	0.9677	0.9334	0.9354	0.9666
10	0.7083	0.4112	0.5438	0.7044	0.7889	0.5764	0.6492	0.7872	0.8140	0.6188	0.6748	0.8055
11	0.8446	0.8316	0.7576	0.8530	0.8750	0.8747	0.8100	0.8902	0.9376	0.9341	0.9047	0.9436
12	0.5371	0.6021	0.5498	0.6791	0.6367	0.6972	0.6489	0.7576	0.5872	0.6661	0.6085	0.7405
13	0.6619	0.3828	0.5927	0.7261	0.6838	0.4331	0.6351	0.7598	0.7146	0.4468	0.6398	0.7710
14	0.7324	0.5573	0.7558	0.8510	0.7595	0.6008	0.7800	0.8670	0.9441	0.8336	0.8938	0.9430
15	0.3938	0.4112	0.4238	0.5692	0.4882	0.5456	0.5220	0.6603	0.5429	0.4746	0.4581	0.6194
16	0.3731	0.1666	0.3175	0.4567	0.4428	0.3044	0.4248	0.5693	0.4802	0.2557	0.3631	0.5227
17	0.8720	0.8327	0.7712	0.8635	0.8596	0.8414	0.7771	0.8708	0.9126	0.8971	0.8503	0.9161
18	0.3144	0.2000	0.3948	0.5270	0.4098	0.4084	0.5404	0.6721	0.4251	0.4819	0.5647	0.7005
19	0.9555	0.9141	0.9192	0.9578	0.9635	0.9201	0.9255	0.9612	0.9813	0.9626	0.9646	0.9819
20	0.8472	0.7448	0.8036	0.8884	0.8333	0.7104	0.7760	0.8715	0.8750	0.7976	0.8375	0.9104
21	0.6589	0.3132	0.4859	0.6536	0.7703	0.5529	0.6350	0.7765	0.7727	0.5026	0.5838	0.7371
22	0.5703	0.7461	0.8307	0.8945	0.6514	0.8025	0.8695	0.9222	0.7719	0.7996	0.8577	0.9187
23	0.6725	0.6481	0.5596	0.6890	0.7304	0.7283	0.6379	0.7545	0.6837	0.6573	0.5809	0.6961
24	0.8566	0.8494	0.7700	0.8649	0.8787	0.8741	0.8010	0.8850	0.8640	0.8595	0.7817	0.8735
25	0.6210	0.6002	0.4560	0.6120	0.7364	0.7291	0.5971	0.7404	0.6901	0.6740	0.5359	0.6873
26	0.7977	0.7954	0.7303	0.8309	0.8391	0.8366	0.7754	0.8662	0.8405	0.8236	0.7638	0.8557
27	0.9579	0.9546	0.9221	0.9589	0.9438	0.9356	0.8919	0.9421	0.9830	0.9821	0.9687	0.9839
28	0.9123	0.9087	0.8525	0.9165	0.9297	0.9292	0.8841	0.9353	0.9429	0.9412	0.9023	0.9468
29	0.8851	0.8731	0.8097	0.8855	0.9154	0.9228	0.8706	0.9234	0.9261	0.9175	0.8686	0.9251
30	0.7821	0.7029	0.5857	0.6402	0.8574	0.9022	0.8436	0.8848	0.9949	0.9935	0.9885	0.9936
Mean	0.6966	0.5886	0.6660	0.7687	0.7669	0.7090	0.7415	0.8345	0.8146	0.7491	0.7720	0.8547
Median	0.7276	0.6109	0.6699	0.7971	0.7903	0.7109	0.7757	0.8661	0.8523	0.7986	0.8187	0.8966
Smallest	0.3144	0.0000	0.3175	0.4567	0.4098	0.3044	0.4248	0.5693	0.4251	0.2557	0.3631	0.5227
Largest	0.9579	0.9546	0.9221	0.9589	0.9635	0.9356	0.9387	0.9653	0.9949	0.9935	0.9885	0.9936

In order to visualize how the proposed method performs in a single dataset, the curves of the balanced accuracies obtained for the datasets `vowel`, `Olivetti_Faces`, `ionosphere`, and `parkinsons` are depicted in Figure 2. The kK -NN classifier is consistently superior compared to both the regular k -NN and adaptive k -NN [LeJeune et al., 2019]. The rationale behind the capacity of the proposed method to improve the regular k -NN may be summarized through three relevant aspects. Firstly, through the use of an adaptive strategy to define neighborhood sizes, the kK -NN is more capable of avoiding both underfitting and overfitting. Secondly, decision boundaries become more adjusted to the samples in regions with higher density, while the boundaries become smoother in regions of lower density. Thus, the classification rule works in an adaptive fashion considering the region of the feature space. Thirdly, high curvature points are commonly related to outliers, being the kK -NN classifier capable of isolating such samples by drastically reducing its neighborhoods - which, consequently, decreases its overall sensitivity to outliers.

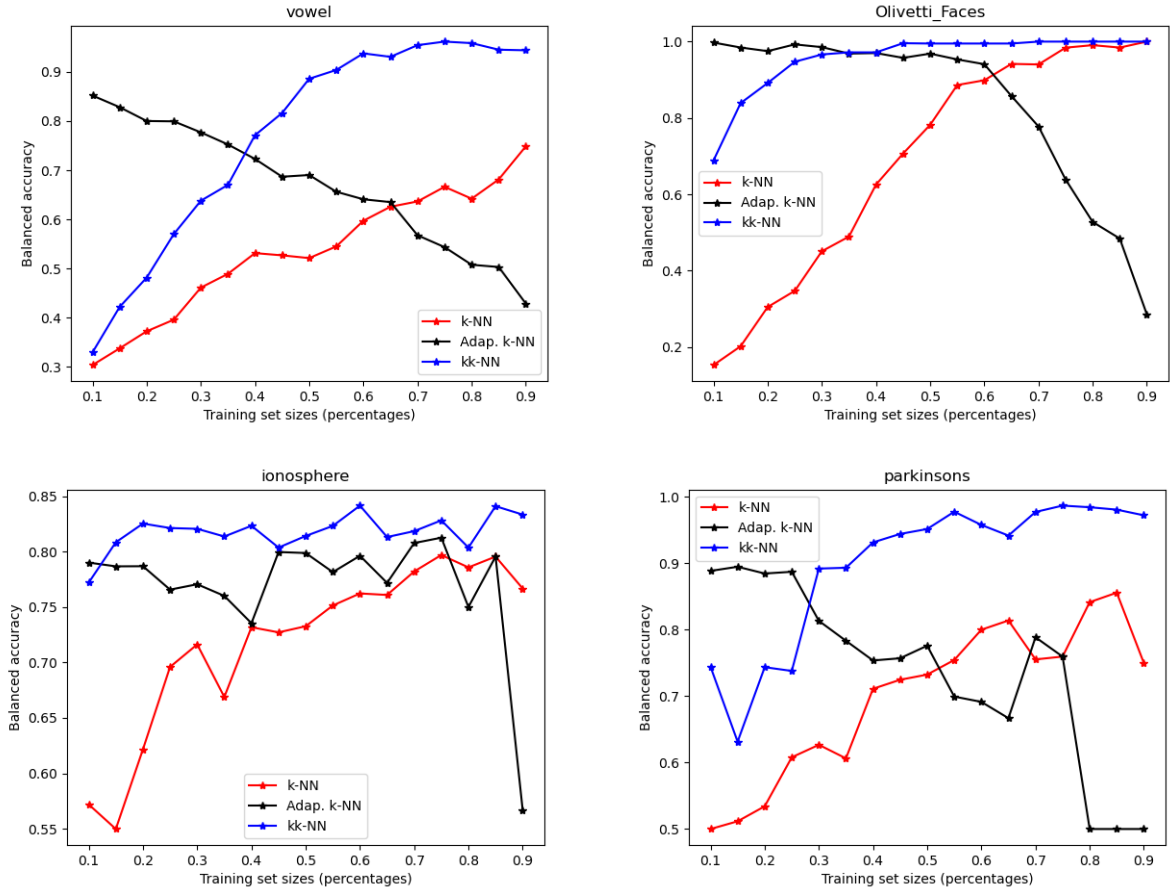


Figure 2: The balanced accuracy curves built by the holdout strategy for the regular k -NN, adaptive k -NN [LeJeune et al., 2019], and the proposed kK -NN classifiers using different partition sizes, from 10% to 90% of the total number of samples. Top-left: vowel dataset. Top-right: Olivetti_Faces dataset. Bottom-left: ionosphere dataset. Bottom-right: parkinsons dataset.

In the second round of experiments, the objective is to compare the performance of all three methods while the training dataset is reduced. The results indicate an interesting feature of the proposed adaptive curvature-based classifier, namely the capacity of the kK -NN to learning from a limited number of samples. The selected datasets and their sample sizes, number of features, and classes are detailed in Table 3.

Table 3: Sample size, number of features, and classes of the selected openML datasets for the second round of experiments.

#	Dataset	# samples	# features	# classes
1	UMIST_Faces_Cropped	575	10304	20
2	variousCancers_final	383	54675	9
3	micro-mass	360	1300	10
4	GCM	190	16064	14

The number of features of all four datasets detailed in Table 3 are substantially larger than the number of samples. Due to the computational complexity of the proposed curvature estimation method, the direct application of the kK -NN classifier is not an option for the raw data. To reduce the number of features, a linear discriminant analysis (LDA) is then applied to extract the maximum possible number of features - i.e., the number of classes minus one.

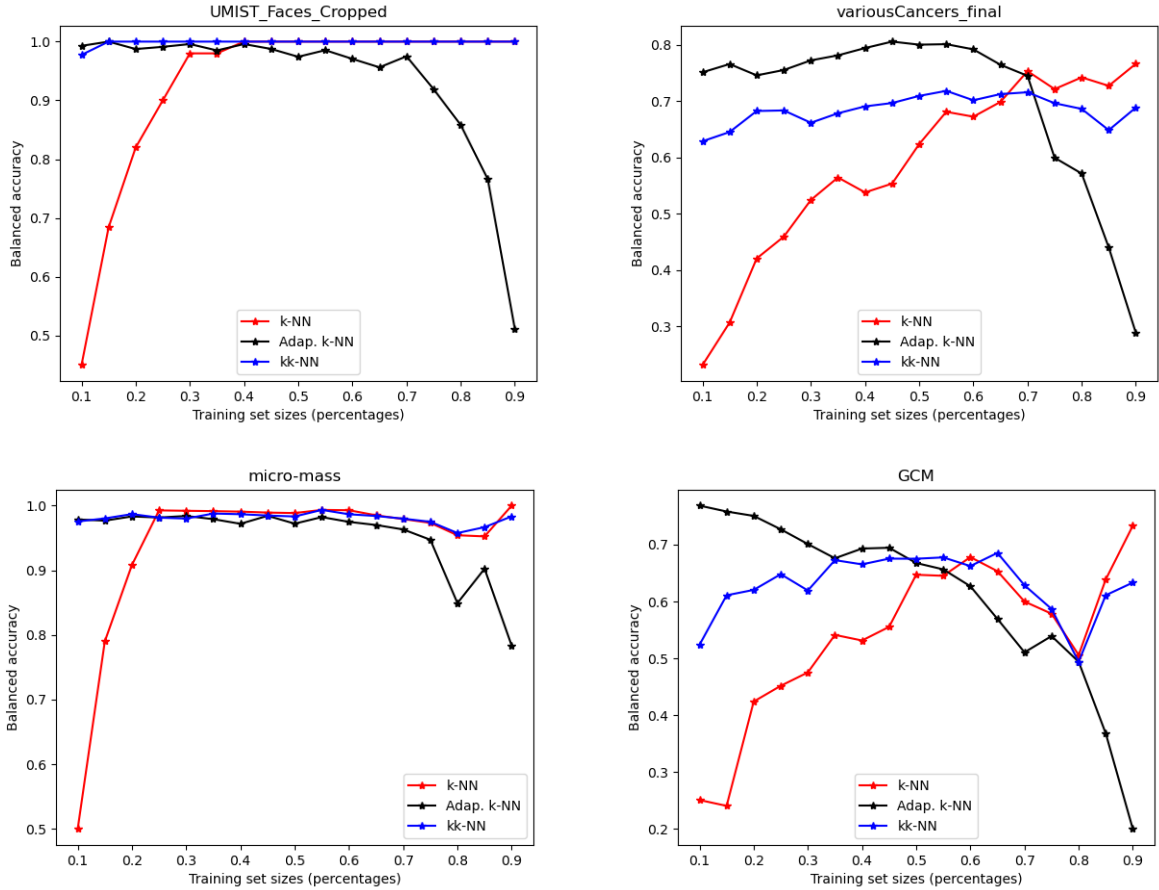


Figure 3: The balanced accuracy curves built by the holdout strategy for the regular k -NN, adaptive k -NN [LeJeune et al., 2019], and the proposed kK -NN classifiers using different partition sizes, from 10% to 90% of the total number of samples. Top-left: UMIST_Faces_Cropped dataset. Top-right: variousCancers_final dataset. Bottom-left: micro-mass dataset. Bottom-right: GCM dataset.

The same strategy adopted in the previous experiment is performed considering four additional datasets, which results are shown in Figure 3. The kK -NN classifier learns more discriminant decision functions while the number of training samples is substantially reduced, indicating that the proposed method may be comparatively more efficient. These results also suggest that the kK -NN algorithm provides more flexible and adjustable decision boundaries while reducing the influence of outliers over the classification process. It is worth noticing that the competing adaptive k -NN algorithm proposed in LeJeune et al. [2019] fails to perform satisfactorily in the case that the testing set is small.

4 Conclusion

In the present work, we introduce a new curvature-based classification method. The kK -NN consists of an adaptive approach to overcome relevant limitations of widely adopted k -NN classification algorithms. The rationale behind the new kK -NN is to adapt the neighborhood size locally, leveraging the curvature information inherent to the dataset in order to improve classification accuracy. Our theoretical analysis and experimental results provide relevant insights into the effectiveness and versatility of the proposed method. Our main findings over 30 real-world datasets may be summarized into three main methodological improvements.

The first methodological improvement concerns a curvature-based adaptation, in which the embodiment of curvature information into the k -NN framework may increase classification performance. By dynamically adjusting the neighborhood size based on the characteristics of the local curvature, the kK -NN is adaptable to different regions of the feature space. The second methodological improvement refers to robustness and generalization. The kK -NN classifier exhibits robustness to noise and outliers, indicating its ability to handle complex and real-world datasets more

effectively. Moreover, the proposed method showcases promising generalization capabilities across different domains, emphasizing its potential for a wide range of applications. Thirdly, extensive experiments exploring many diverse datasets indicate that the kK -NN outperforms established k -NN classifiers in various scenarios. The adaptive nature of the kK -NN enables it to excel in situations where the local density of samples and curvature patterns vary significantly.

Therefore, the adaptive curvature-based approach adopted in the kK -NN introduces a promising advancement within k -NN classification methods. Empirical analyses provide evidence of its efficacy considering diverse scenarios, indicating relevant possibilities for future research and applications in machine learning (e.g., pattern recognition, computer vision). The incorporation of curvature information into classification frameworks offers a nuanced perspective that unfolds new possibilities for enhancing the adaptability and robustness of classification algorithms.

Suggestions of future extensions include additional theoretical investigations into the properties of curvature-adaptive classifiers, further exploring its underlying mechanisms. Analyzing the convergence properties and establishing theoretical bounds on the performance of kK -NN under different conditions would contribute to the theoretical foundations of the curvature-based classification. Moreover, the curvature-based adaptation of the kK -NN could be applied to image processing tasks, particularly in scenarios where local variations and intricate data patterns play a crucial role. Lastly, considering that the principles underlying the kK -NN are rooted in curvature analysis, the proposed method may find applications in dimensionality reduction and metric learning.

Statements and declarations

Funding

This study is partially funded by the the Coordination for the Improvement of Higher Education Personnel (CAPES), Brazil - Finance Code 001.

Code availability

Python scripts to reproduce the results reported in this paper may be found at <https://github.com/aalexandrelevada/kkNN>. The implementation is a first version prototype of the proposed kK -NN algorithm, which is not optimized for best performance. Most functions may be further improved to reduce computational time.

Data availability

All datasets used in the experiments are publicly available at www.openml.org.

References

- T. Cover and P. Hart. Nearest neighbor pattern classification. *IEEE Transactions on Information Theory*, 13(1):21–27, 1967. doi: 10.1109/TIT.1967.1053964.
- Frank Nielsen. Supervised learning: practice and theory of classification with the k -NN rule. In *Introduction to HPC with MPI for Data Science*, pages 213–229. Springer, Switzerland, 2016.
- S. Zhang. Challenges in KNN Classification. *IEEE Transactions on Knowledge & Data Engineering*, 34(10):4663–4675, oct 2022. doi: 10.1109/TKDE.2021.3049250.
- Panos K. Syriopoulos, Nektarios G. Kalampalikis, Sotiris B. Kotsiantis, and Michael N. Vrahatis. kNN Classification: a review. *Annals of Mathematics and Artificial Intelligence*, 2023. doi: 10.1007/s10472-023-09882-x.
- Danilo Samuel Jodas, Leandro Aparecido Passos, Ahsan Adeel, and João Paulo Papa. PL-k NN: A Parameterless Nearest Neighbors Classifier. In *2022 29th International Conference on Systems, Signals and Image Processing (IWSSIP)*, volume CFP2255E-ART, pages 1–4, 2022. doi: 10.1109/IWSSIP55020.2022.9854445.
- Shahadat Uddin, Ibtisham Haque, Haohui Lu, Mohammad Ali Moni, and Ergun Gide. Comparative performance analysis of K -nearest neighbour (KNN) algorithm and its different variants for disease prediction. *Scientific Reports*, 12(1):6256, 2022. doi: 10.1038/s41598-022-10358-x.
- Gustavo E.A.P.A. Batista and Diego Furtado Silva. How k -nearest neighbor parameters affect its performance. In *Proceedings of the 38th Argentine Symposium on Artificial Intelligence (ASAI 2009)*, pages 95–106, 2009.
- Haneen Arafat Abu Alfeilat, Ahmad BA Hassanat, Omar Lasassmeh, Ahmad S Tarawneh, Mahmoud Bashir Alhasanat, Hamzeh S Eyal Salman, and VB Surya Prasath. Effects of distance measure choice on k-nearest neighbor classifier performance: a review. *Big data*, 7(4):221–248, 2019.

- Puning Zhao and Lifeng Lai. Efficient Classification with Adaptive KNN. In *Proceedings of the 35th AAAI Conference on Artificial Intelligence (AAAI-21)*, volume 35, pages 11007–11014, 2021.
- Merkourios Papanikolaou, Georgios Evangelidis, and Stefanos Ougiaroglou. Dynamic k determination in k -NN classifier: A literature review. In *2021 12th International Conference on Information, Intelligence, Systems & Applications (IISA)*, pages 1–8, 2021. doi: 10.1109/IISA52424.2021.9555525.
- Raja Sakti Arief Daulay, Syahril Efendi, and Suherman. Review of Literature on Improving the KNN Algorithm. *Transactions on Engineering and Computing Sciences*, 11(3):63–72, Jun. 2023. doi: 10.14738/tecs.113.14768.
- Shiliang Sun and Rongqing Huang. An adaptive k -nearest neighbor algorithm. In *2010 Seventh International Conference on Fuzzy Systems and Knowledge Discovery*, volume 1, pages 91–94, 2010. doi: 10.1109/FSKD.2010.5569740.
- Zizhu Fan, Yijing Huang, Chao Xi, and Qiang Liu. Multi-view adaptive k -nearest neighbor classification. *IEEE Transactions on Artificial Intelligence*, pages 1–14, 2023. doi: 10.1109/TAI.2023.3296092.
- Manfredo P. do Carmo. *Differential Geometry of Curves and Surfaces*. Dover Publications Inc., New York, 2nd edition, 2017.
- Tristan Needham. *Visual Differential Geometry and Forms: A Mathematical Drama in Five Acts*. Princeton University Press, Princeton, 2021.
- Jean-Daniel Boissonnat and Mathijs Wintraecken. The topological correctness of PL approximations of isomanifolds. *Found. Comput. Math.*, 22(4):967–1012, 2022. doi: 10.1007/S10208-021-09520-0. URL <https://doi.org/10.1007/s10208-021-09520-0>.
- Daniel LeJeune, Reinhard Heckel, and Richard Baraniuk. Adaptive estimation for approximate k -nearest-neighbor computations. In *The 22nd International Conference on Artificial Intelligence and Statistics*, pages 3099–3107. PMLR, 2019.
- D. Eppstein, M.S. Paterson, and F.F. Yao. On nearest-neighbor graphs. *Discrete and Computational Geometry*, 17: 263–282, 1997.
- Dewei Li and Yingjie Tian. Survey and experimental study on metric learning methods. *Neural Networks*, 105:447–462, 2018. ISSN 0893-6080.
- Fei Wang and Jimeng Sun. Survey on distance metric learning and dimensionality reduction in data mining. *Data Min. Knowl. Discov.*, 29(2):534–564, March 2015. ISSN 1384-5810. doi: 10.1007/s10618-014-0356-z.
- Joseph F. Hair-Jr., William C. Black, Barry J. Babin, and Rolph E. Anderson. *Multivariate Data Analysis*. Cengage, New York, 8 edition, 2018.
- Wolfgang Kuhnel. *Differential Geometry: Curves - Surfaces - Manifolds*. American Mathematical Society, New York, 3 edition, 2015.
- Hunter S Chase. Fundamental forms of surfaces and the gauss-bonnet theorem. *University of Chicago, Chicago*, 2012.
- David L. Donoho and Carrie Grimes. Hessian eigenmaps: Locally linear embedding techniques for high-dimensional data. *Proceedings of the National Academy of Sciences*, 100(10):5591–5596, 2003.
- Loring W Tu. *Differential geometry: connections, curvature, and characteristic classes*, volume 275. Springer, 2017.
- John Oprea. *Differential Geometry and its Applications*. The Mathematical Association of America, New York, 2 edition, 2007.
- A. N. Gorban and I. Y. Tyukin. Blessing of dimensionality: mathematical foundations of the statistical physics of data. *Philosophical Transactions of the Royal Society of London Series A*, 376(2118):20170237, April 2018.
- Charles Fefferman, Sanjoy Mitter, and Hariharan Narayanan. Testing the manifold hypothesis. *Journal of the American Mathematical Society*, 29(4):983–1049, October 2016.
- John Nash. The imbedding problem for riemannian manifolds. *Annals of mathematics*, 63(1):20–63, 1956.
- Bang-yen Chen. *Geometry of submanifolds*. Courier Dover Publications, New York, 2019.
- Alper Yilmaz and Mubarak Shah. Actions sketch: A novel action representation. In *2005 IEEE Computer Society Conference on Computer Vision and Pattern Recognition (CVPR'05)*, volume 1, pages 984–989. IEEE, 2005.
- Kashvi Taunk, Sanjukta De, Srishti Verma, and Aleena Swetapadma. A brief review of nearest neighbor algorithm for learning and classification. In *2019 International Conference on Intelligent Computing and Control Systems (ICCS)*, pages 1255–1260, 2019. doi: 10.1109/ICCS45141.2019.9065747.
- Andrew R. Webb and Keith D. Copesey. *Statistical Pattern Recognition*. John Wiley & Sons, London, 3 edition, 2011.
- Quentin Mérigot, Maks Ovsjanikov, and Leonidas J Guibas. Voronoi-based curvature and feature estimation from point clouds. *IEEE Transactions on Visualization and Computer Graphics*, 17(6):743–756, 2010.

- Scott Fortmann-Roe. Understanding the bias variance tradeoff . <https://scott.fortmann-roe.com/docs/BiasVariance.html>, 2012.
- Wojciech Jarosz. *Efficient Monte Carlo methods for light transport in scattering media*. University of California, San Diego, 2008.
- Don O Loftsgaarden and Charles P Quesenberry. A nonparametric estimate of a multivariate density function. *The Annals of Mathematical Statistics*, 36(3):1049–1051, 1965.
- George R Terrell and David W Scott. Variable kernel density estimation. *The Annals of Statistics*, pages 1236–1265, 1992.

Appendices

A Shape operator and curvatures

Differential geometry provides a framework to study properties that are invariant under smooth mappings, preserving differentiability. It focuses on studying geometric objects such as curves and surfaces, while understanding their properties regarding differential calculus [do Carmo, 2017, Needham, 2021]. Potential applications across various domains include physics, engineering, computer science, robotics, among many more. In physics, it is applied to describe the geometry of spacetime in general relativity, whereas in computer graphics it is employed to model and manipulate smooth surfaces [Tu, 2017]. The mathematical concepts and tools of differential geometry provide a powerful framework to understand the intrinsic geometry of spaces as well as their applications to diverse fields of knowledge [Oprea, 2007]. The notion of surface in \mathbb{R}^3 is generalized to higher dimensions by the definition of manifold.

Definition 1 (Manifold). *Let M be a topological space. Then, M is an n -dimensional smooth manifold if it satisfies the following conditions:*

- **Locally Euclidean:** *For every point $p \in M$, there exists an open neighborhood U of p such that U is homeomorphic to an open subset of \mathbb{R}^n . Formally, there exists a homeomorphism $\phi : U \rightarrow V$, where V is an open subset of \mathbb{R}^n .*
- **Smoothness:** *The collection of such local homeomorphisms ϕ forms an atlas on the manifold M . A smooth manifold M is equipped with a smooth structure, which consists of an atlas which transition maps (i.e., maps between overlapping neighborhoods) are all smooth, meaning that they have continuous derivatives of all orders.*
- **Hausdorff and second-countable:** *The manifold M is required to be a Hausdorff space, meaning that for any two distinct points in M there exist disjoint open sets containing each point. Moreover, M must be second-countable, which means that its topology has a countable basis.*

Manifolds consist of a fundamental framework for studying spaces with intrinsic geometry, finding applications in many areas of mathematics, including data analysis and machine learning, where they are employed to model complex datasets and high-dimensional spaces [Gorban and Tyukin, 2018, Fefferman et al., 2016].

A tangent space is a fundamental concept in differential geometry, providing an understanding of the local behavior of a manifold at a particular point. The tangent space to a manifold at a point captures the notion of “infinitesimal” directions at that point. Tangent vectors represent directions and rates of change at a point on the manifold. Intuitively, in a smooth surface such as a sphere or curve, the tangent vectors at a particular point represent possible directions to move along the surface or the direction of velocity if it is passing through that point.

Definition 2 (Tangent space). *Let M be a smooth manifold and p a point in M . The tangent space T_pM to M at p is defined as the set of all tangent vectors at p .*

- **Basis of tangent space:** *The tangent space T_pM is a vector space, which basis consisting of tangent vectors corresponding to coordinate curves passing through p . In local coordinates, these basis vectors are frequently denoted as $\partial/\partial x^i$, where i ranges over the n dimensions of the manifold M .*

The tangent space captures the local geometry of the manifold at a specific point, being instrumental in defining notions such as tangent bundles, differential forms, and differential operators on manifolds. The metric tensor (also known as the first fundamental form) is another mathematical object that plays an important role in the computation of inner products and arc lengths in a manifold.

Definition 3 (First fundamental form or metric tensor). *Let M be a smooth manifold. The first fundamental form on M , denoted by \mathbb{I} or g , is a smoothly varying collections of inner products defined on the tangent spaces of M , such that for each point $p \in M$ the metric tensor defines an inner product g_p to the tangent space T_pM . The metric tensor g is a symmetric, non-degenerate, and smoothly varying bilinear form on the tangent bundle of the manifold. Therefore, for any two tangent vectors X, Y at a point p on M , the metric tensor g assigns a real number $g_p(X, Y)$ that satisfies:*

- **Symmetry:** $g_p(X, Y) = g_p(Y, X)$ for all the tangent vectors at p .

- **Linearity:** g_p is linear in each argument, thus for any tangent vectors X, Y, Z and scalars α, β , we have:

$$g_p(\alpha X + \beta Y, Z) = \alpha g_p(X, Z) + \beta g_p(Y, Z) \quad (9)$$

$$g_p(X, \alpha Y + \beta Z) = \alpha g_p(X, Y) + \beta g_p(X, Z) \quad (10)$$

- **Non-degeneracy:** The metric tensor is non-degenerate, meaning that for any non-zero tangent vector X at p , there exists another tangent vector Y such that $g_p(X, Y) \neq 0$.

Intuitively, the first fundamental form enables the computation of distances along the paths within the surface. It is known as an intrinsic metric due to the fact that it is a Riemannian metric of the manifold. The second fundamental form of a manifold is a geometric object that characterizes the extrinsic curvature of a submanifold within a higher-dimensional manifold. This is also known as the Euler-Schouten embedding curvature. Commonly, the submanifold M with m dimensions is embedded in an Euclidean space \mathbb{R}^n , with $n > m$. This refers to the Nash embedding theorems [Nash, 1956].

The second fundamental form is a pivotal instrument in the study of submanifolds [Chen, 2019], providing important geometric information about their shape and curvature within the ambient manifold. It plays a significant role in various areas of mathematics, including differential geometry, geometric analysis, mathematical physics, and computer vision [Yilmaz and Shah, 2005].

Definition 4 (Second fundamental form). *Let M be a smooth manifold. The second fundamental form of M , denoted by \mathbb{III} , is a bilinear form defined on the tangent space of M at each point. Basically, it is related to the curvature of the normal section along a direction \vec{v} at the point p . In simpler terms, it measures how curved the trajectory should be if it is moving along the direction \vec{v} . The second fundamental form reveals how fast the manifold moves away from the tangent plane.*

The second fundamental form describes how curved the embedding is, indicating how the manifold is located within the ambient space. It is a type of derivative of the unit normal along the surface. Equivalently, it is the rate of change of the tangent planes taken in various directions, consisting of an extrinsic quantity.

Definition 5 (Shape operator and curvatures). *The shape operator of a manifold M with first fundamental form \mathbb{I} and second fundamental form \mathbb{III} is given by $P = -\mathbb{III} \cdot \mathbb{I}^{-1}$.*

- The Gaussian curvature K_G is the determinant of the shape operator P .
- The mean curvature K_M is the trace of the shape operator P .
- The principal curvatures are the eigenvalues of the shape operator P .

Considering the definitions above, we introduce an algorithm for curvature estimation through a nonparametric approximation for the shape operator. This new algorithm adopts local curvatures to adjust the neighborhoods within the k -NN classifier through an adaptive approach.

B The k -nearest neighbor classifier

The k -NN classifier is a simple and effective algorithm employed in supervised learning. It belongs to the family of instance-based learning or lazy learning methods, where the algorithm does not build an explicit model during the training phase. Instead, it memorizes the entire training dataset to perform predictions based on the similarity of new instances compared to the training dataset [Taunk et al., 2019].

The k -NN may be understood as the Bayesian classifier when the densities of the conditional class are estimated using a nonparametric approach [Webb and Copley, 2011]. The probability of a sample \vec{x} be in a region of interest of volume $V(\vec{x})$, centered on \vec{x} is given by:

$$\theta = \int_{V(\vec{x})} p(\vec{x}) d\vec{x} \quad (11)$$

which is a generalization of the area under the curve defined by the probability density function (PDF). In the case of multiple dimensions, a volume is calculated instead of an area. However, for a small volume $V(\vec{x})$, we have the following approximation:

$$\theta \approx p(\vec{x})V(\vec{x}) \quad (12)$$

as the the volume of the box may be computed as the volume of the region times the height (i.e., probability). The probability θ may be approximated by the proportion of samples that belong to the region of volume $V(\vec{x})$. In the case there are k samples from a total of n that belong to such a region, then:

$$\theta \approx \frac{k}{n} \quad (13)$$

which is a proportion and, therefore, it belongs to the interval $[0, 1]$. Combining equations 12 and 13, the following approximation for $p(\vec{x})$ is found:

$$p(\vec{x}) = \frac{k}{nV(\vec{x})} \quad (14)$$

Hence, the conditional probability of the class ω_j in a nonparametric manner may be estimated:

$$p(\vec{x}|\omega_j) = \frac{k_j}{n_j V_R} \quad (15)$$

where k_j denotes the number of samples in class ω_j in the region of interest, n_j denotes the total number of samples in class ω_j , and V_R represents the volume of the region of interest. Similarly, the prior probability of class ω_j is given by:

$$p(\omega_j) = \frac{n_j}{n} \quad (16)$$

where n denotes the total number of samples. Therefore, by the maximum a posteriori criterion (MAP), we must assign the sample \vec{x} to the class ω_j if:

$$p(\omega_j|\vec{x}) > p(\omega_i|\vec{x}) \quad \forall i \neq j \quad (17)$$

which leads to:

$$\frac{k_j}{n_j V_R} \frac{n_j}{n} > \frac{k_i}{n_i V_R} \frac{n_i}{n} \quad \forall i \neq j \quad (18)$$

and after some simplifications, it is reduced to:

$$k_j > k_i \quad \forall i \neq j \quad (19)$$

This means that the sample \vec{x} should be assigned to the most representative class in its k nearest neighbors. Algorithms 4 and 5 detail the pseudocodes of the regular k -NN classifier.

Algorithm 4 Get the k nearest neighbors of a sample

```

function GET_NEIGHBORS(train_set, test_row, k)
  distances  $\leftarrow$  [ ]
  indices  $\leftarrow$  [ ]
  for each train_row in train_set do
    dist  $\leftarrow$  EuclDist(test_row, train_row[:-1])
    distances.append(train_row)
  end for
  Sort the tuples in distances in ascending order of dist
  neighbors  $\leftarrow$  [ ]
  for ( $i = 0; i < k; i++$ ) do
    neighbors.append(distances[i][0])
  end for
  return neighbors
end function

```

▷ Last feature is the class label

Algorithm 5 k -NN classification

```

function KNN_CLASSIFICATION(train_set, test_row, k)
  neighbors  $\leftarrow$  get_neighbors(train_set, test_row, k)
  labels  $\leftarrow$  [row[-1]] for row in neighbors
  prediction  $\leftarrow$  mode(labels)
  return prediction
end function

```

▷ Last feature is the label
▷ The label that occurs most often

It has been reported that the probability of error in the k -NN classifier is directly related to the probability of error in the Bayesian classifier - which is the lowest among supervised classifiers [Cover and Hart, 1967]:

$$P_{knn} \leq P^* \left(2 - \frac{c}{c-1} P^* \right) \quad (20)$$

where c denotes the number of classes, and P^* is the probability of error in the Bayesian classifier. Moreover, it is worth noticing that there is an intrinsic relation between the k -NN classifier and Voronoi tessellation. This relation lies in their geometric interpretation as well as adoption of partitioning the feature space [Mérigot et al., 2010]. An example of a Voronoi diagram in the partition of an 2D feature space is depicted in Figure 4 - originally from [Fortmann-Roe, 2012].

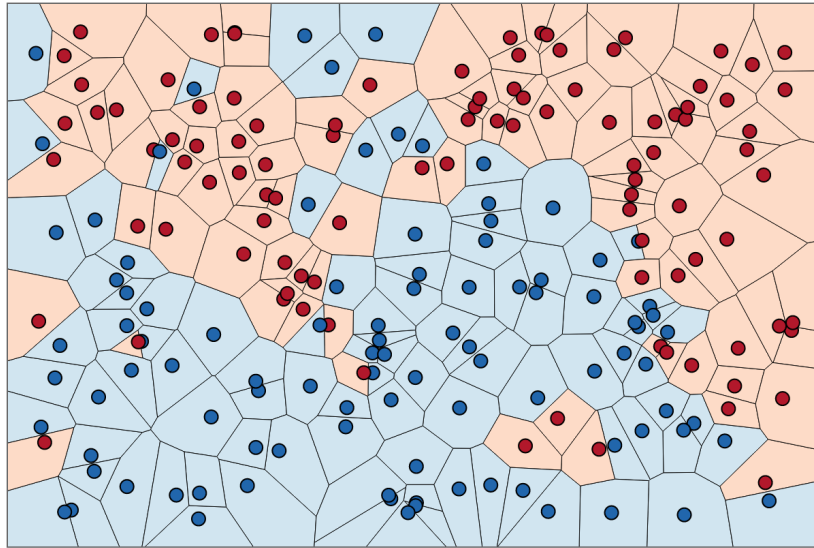


Figure 4: The k -NN decision boundary and the Voronoi tessellation in an 2D feature space [Fortmann-Roe, 2012]

The decision boundary obtained by the k -NN classifier is the union of several piece-wise linear edges of the Voronoi tessellation, which frequently leads to a complex nonlinear behavior.

B.1 Balloon and sample-point estimator

In general, the degree of smoothing applied to the data is determined by a bandwidth. The underlying PDF is smoothed as a consequence of a larger bandwidth, which decreases the variance while increasing the bias. On the other hand, if the bandwidth is reduced, the variance increases although the bias reduces. Selecting the ideal bandwidth is frequently difficult without understanding the true underlying PDF. Adopting only one bandwidth may provide suboptimal results when considering the whole domain. This approach may induce to oversmoothing in high density neighbourhoods.

Conversely, in cases of small sample sizes, it may lead to undersmoothing in the neighbourhood of the extreme regions of the distribution (tails). Without a relevant understanding of the density function, it is challenging to select the ideal bandwidth. To mitigate this issue, locally adaptive approaches empower the bandwidth to vary over the domain of the PDF [Jarosz, 2008]. One of such locally adaptive approaches refers to the balloon estimator, which was originally proposed as a k -NN estimator [Loftsgaarden and Quesenberry, 1965]. A general form of the balloon estimator is detailed as:

$$\hat{p}(\vec{x}) = \frac{1}{Nh(\vec{x})} \sum_{i=0}^{N-1} K \left[\frac{\vec{x} - \vec{x}_i}{h(\vec{x})} \right] \quad (21)$$

where N is the number of samples, $h(\vec{x})$ is the bandwidth as a function of \vec{x} , and K refers to its kernel. The issue of selecting bin locations is addressed by the kernel estimator, which generalizes the naive estimator to remove discontinuities of the corresponding PDF. Nonetheless, the balloon estimator is subject to several inefficiencies, particularly regarding univariate data. Whether applied globally, its estimate commonly does not integrate to one over the domain. An additional issue refers to the fact that the bandwidth consists of a discontinuous function, which affects the associated PDF [Terrell and Scott, 1992].

A further local bandwidth estimator is the sample-point estimator, which general form is detailed as:

$$\hat{p}(\vec{x}) = \frac{1}{N} \sum_{i=0}^{N-1} \frac{1}{h(\vec{x}_i)} K \left[\frac{\vec{x} - \vec{x}_i}{h(\vec{x}_i)} \right] \quad (22)$$

The difference between the balloon and sample-point estimator lies in the bandwidth $h(\vec{x}_i)$, which is a function of \vec{x}_i instead of \vec{x} . In the sample-point estimator approach, every data point is assigned a kernel. However, the size of such kernels may change across data points. The sample-point estimator exhibits advantages compared to the balloon estimator. Considering that each kernel is normalized, the estimator consists of an PDF that integrates to one. Lastly, the sample-point estimator may be entirely continuous due to the fact that it adopts the differential attributes of the respective kernel functions [Jarosz, 2008].